

## **Advanced Process for Turbine blades to improve the efficiency of the Wind Turbine System.**

Department of mechanical and mechanics, Dr. Praful Patel, Government Engineering college, surat  
Email-patelprafurina@gmail.com

### **Abstract**

*The objective of this article is to develop the system in the planning of turbine edges and generator to extend the capability of a wind turbine. Hydrodynamic reenactment of turbine edges and the reason setting of the controller are constantly focused on securing most extraordinary power from the turbine framework. Inspect on the organizing of the two systems, turbine bleeding edges and the generator, is exceptional. If turbine edges are not at first especially organized with the generator, the perfect arrangement of the turbine front lines to accomplish peak execution won't be recognized, and the controller will be remarkable augmentation the control gets. Subsequently, the planning issue is meriting being discussed. In this article, the profitability of the wind turbine framework is extended by choosing the perfect relentless voltage technique for the generator. As the ideal consistent voltage mode is chosen, the qualities of the working focuses, for example, tip speed proportion, cycles every moment, cutting edge torque, furthermore, productivity, can be distinguished by the hybrid purpose of the  $T$  (torque)– $N$  (r/min) bends of the turbine sharp edges and the generator. An even upwind turbine is dealt with as the study case here. It is recommended that the tip speed proportion esteem figured by the decided cycles every moment ought to be situated in the high-productivity area of effectiveness bends of the turbine sharp edges, however not in the lofty incline locale of the chose consistent voltage method of the generator. The comes about demonstrate that, if the two systems work well, the last yield control at a low twist speed of 4–5 m/s will be expanded by 65%–44%, and at a high twist speed of 10–12 m/s, it will be expanded by 3%–5%.*

**Keywords:** *Computational liquid progression, turbine edges, generator, even upwind turbine, tip speed proportion, steady voltage mode*

## INTRODUCTION

Since the 2000s, much consideration has been paid to acquiring renewable vitality from the wind. From 2008 to 2014, the worldwide electric wind limit developed by a normal yearly rate of 20.9%. Look into techniques received to concentrate how to pick up the greatest power from the turbine system by and large have focused on the hydrodynamic recreation of turbine cutting edges and the rationale setting of the controller; coordinating the two systems, the turbine sharp edges and the generator, is moderately uncommon. In an inadequately coordinated turbine system, the lessening in effectiveness is generally more than 15%. This study explores the usage of coordinating systems that will enhance the effectiveness of the wind turbine system.

Appropriately, a coordinating procedure will be developed. Traditionally, turbine sharp edges were planned agreeing to sharp edge component force (BEM), as talked about in Glauert.<sup>1</sup> Dynamic slow down rectifications were embraced by Leishman<sup>2</sup> to enhance BEM hypothesis. Be that as it may, the collaboration of rotational stream and three-dimensional (3D) sharp edges were not portrayed unmistakably by BEM. Along these lines, the expectation of execution by BEM

leaves much to be craved. Hirsch<sup>3</sup> connected computational liquid elements (CFD) in sharp edge reproduction. Bardina et al.<sup>4</sup> remarked that the shear-stretch transport (SST)  $k-\epsilon$  turbulence demonstrate determined by the Menter<sup>5</sup> was appropriate for anticipating the streams with partition under antagonistic weight angles. Fingersh et al.<sup>6</sup> and Hand et al.<sup>7</sup> led streamlined examinations of turbine sharp edges in wind burrows and gave profitable test information to 3D CFD rotor investigations. Sørensen et al.<sup>8</sup> settled the Navier–Stokes condition for wind turbines utilizing the multi-square limited volume strategy and brought about understanding with test estimations. Johansen et al.<sup>9</sup> utilized an incompressible Reynolds-averaged at the midpoint of Navier–Stokes (RANS) solver to figure the rotor edges, by applying a multi-piece, organized work and a segregated whirlpool reproduction; notwithstanding, slow down start at 10 m/s wind speed was not caught. It was apparent in al.<sup>10</sup> that stream over pivoting cutting edges is significantly unique in relation to the stream over a wing, and 3D reenactments can't be supplanted by two-dimensional (2D) reenactments. In Tongchitpakdee et al.,<sup>11</sup> the yawed stream conditions were incorporated into the CFD reenactments. Three diverse time-precise inviscid CFD

recreations had been processed for the two-bladed wind turbine utilizing a limited volume stream solver with turning unstructured tetrahedral systems in Sezer-Uzol and Long.<sup>12</sup> In SezerUzol what's more, Long,<sup>12</sup> sectional weight coefficient circulations concurred well with trial information; be that as it may, the stream partition couldn't be portrayed due to the in viscid character. Huang et al.<sup>13</sup> utilizing a non-inertial reference outline talked about the streamlined marvel of pivoting cutting edges. In C Van Dam,<sup>14</sup> it was finished up that CFD reenactments for wake improvement were basically influenced by lattice, and wake improvement was fundamentally influenced by the turbine rotor tip speed proportion (TSR) and streamlined stacking. Dynamic overset network innovation for CFD reproduction was exhibited in Li et al.<sup>15</sup> for calculation of bodies with relative movements, including versatile disfigurement. In Villalpando et al.,<sup>16</sup> the streamlines around the clean and frosted airfoil were dissected to assess the ice affect on lift and drag with the SST k2v display. The execution of a turbine cutting edge with an extensive driving edge width and wedge point was explored in Sun et al.<sup>17</sup> Yelmule furthermore, EswaraRao Anjuri<sup>18</sup> is a contextual investigation in which the capacity of

CFD in foreseeing complex 3D wind turbine streamlined features was shown with NREL Stage VI information. As indicated by Chamorro and Arndt,<sup>19</sup> the wind turbine is displayed as an actuator disk, without considering the pivot of the wake. Boussinesq and Coriolis adjustment elements are connected in the direct force and vitality conditions to represent the impacts of the non-uniform speed dissemination. In Johnson et al.,<sup>20</sup> a CFD actuator circle model was directed to include distinctive limit conditions, including a channel and conduit stream.

The demonstrate indicated great concurrence with the onedimensional (1D) force hypothesis as far as speed also, weight profiles. Kosasih and Hudin<sup>21</sup> enhanced the execution of the turbine system by recognizing turbulence power. Yin et al.<sup>22</sup> broke down the system plan, essential element qualities, warm misfortunes, and administration perspectives; hydro-thick transmission was connected to upgrade the general productivity. The impedance of wind turbine surge movement was talked about in Tran and Kim<sup>23</sup> as a consequence of CFD and sharp edge component energy (BEM) examinations. Koutroulis and Kalaitzakis<sup>24</sup> connected the Perturb furthermore, Observe Algorithm to track

the most extreme power of the turbine system by the controller. Mireckiet al.<sup>25</sup> set Fuzzy Logic in the controller to acquire most extreme control. As indicated by Odgaard et al.,<sup>26</sup> multi-objective display prescient control (MPC) issues are tuned utilizing Pareto bends to minimize the cost of vitality of the wind turbine system.

In this article, we demonstrate that the effectiveness of the wind turbine is enhanced by coordinating the turbine sharp edges and the generator. A level upwind turbine is registered by CFD innovation and afterward coordinated with the chose generator. Both coordinated and unmatched results will be analyzed to demonstrate the change in the last effectiveness test.

### Scientific model

The optimal design of this study case is examined utilizing the business CFD programming, ANSYS Familiar. The SST k- $\nu$  turbulence model of the second-arrange upwind plan with the SIMPLE calculation technique is connected to settle the RANS conditions.

The time averaging approach for a period subordinate and sporadic movement parts all the time differing terms into mean and

fluctuating qualities. ANSYS Fluent settles the RANS conditions by limited volume discretization. The SST k- $\nu$  display presented by Menter<sup>27</sup> is connected in this article. To gauge unfavorable weight inclinations, airfoils, also, transonic stun waves, the SST k- $\nu$  display has been emphatically prescribed by Menter.<sup>28</sup> The straightforward calculation determined by Patankar and Spalding<sup>29</sup> was utilized to comprehend the incompressible stream. The principle thought of this plan is to overhaul the weight what's more, speeds by adjusted terms. Li et al.<sup>15</sup> said that the stream in wind turbines is still basically incompressible with Mach numbers in light of a cutting edge tip speed infrequently surpassing 0.25. The Mach numbers in view of the cutting edge tip speed in this study did not surpass 0.25; accordingly, it was sensible to consider the stream as incompressible in this article.



*Fig 1. The outline of wind turbine.*

**Fitting course of action and limit conditions -**

As indicated by Wuřow et al.,<sup>30</sup> with a specific end goal to accurately investigate the relative speed of a turning turbine, two registering spaces are important: one encases the figured structures, and the other one incorporates the entirety figuring space. In this manner, the inward and external spaces are both created in the present calculation.

**Table 1.** The associative specifications of the discussed wind turbine.

Rated power (W @ m/s)	3000 @ 12
Rotor diameter (m)	3.7
Number of blades	3
Foil type of blades	S826
Root twist angle of blades (°)	23
Root chord length of blades (mm)	266
Blade material	Fiberglass
Rated speed (r/min)	350
Swept area (m <sup>2</sup> )	10.8
Start-up wind speed (m/s)	3
Cut-in wind speed (m/s)	3.5
kWh per year (m/s)	5000 @ 6
Body	Cast aluminum
Overspeed protection	Electronic torque control
Weight (kg)	82

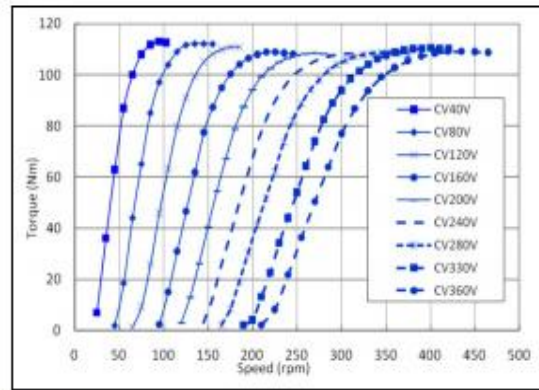


**Figure 2.** The T–N curves of this generator tested by CV model.

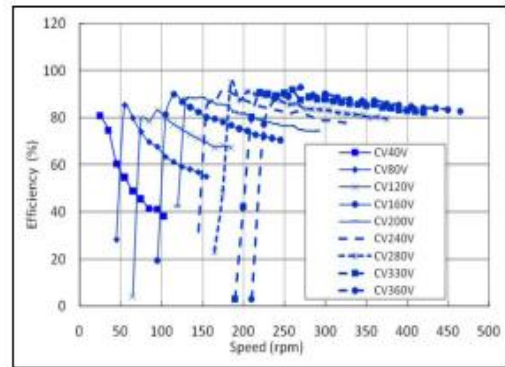


**Figure 3.** The efficiency of this generator.

The size model was developed. One turbine sharp edge and 33% of the center point and turbine edge are encased in the inward area. The span of the turbine sharp edge is noted by R. The bay of the external area is situated at 6R upstream of the inward area, and the outlet is situated at 12R downstream of the internal space. The remove from the turbine sharp edge hub to the outer domain chamber surface is 6R. The measure of the internal space is made to fit the included structures.

**Table 2.** The  $C_p$  comparison between the measured and calculated values.

	Wind speed (m/s)	Rotating speed (r/min)	$C_p$ (%)
By CFD (1.6 M cells)	10	251	34
By farm test	10	251	34.3

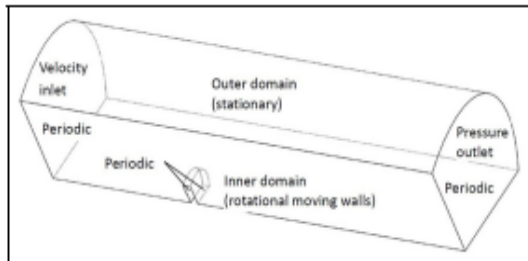


**Fig 4.** Applied Boundary Conditions.

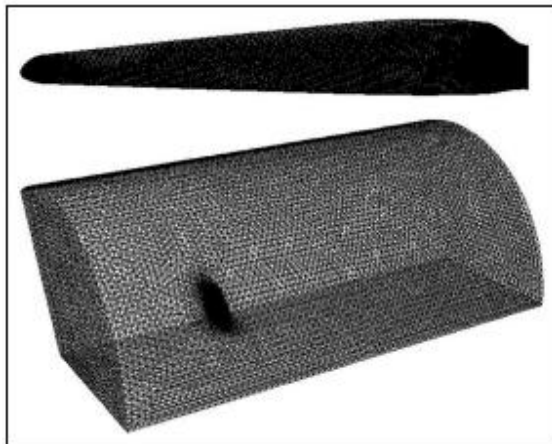


**Fig 5.** The arranged meshes for the present case.

## RESULTS AND DISCUSSION

The situation while coordinating the turbine cutting edges with the generator. In this article, the considered wind rates are 4, 5, 6, 8, 10, and 12 m/s. For each wind speed, the calculations are directed from low speed to rapid. The recreations by CFD are coordinated with the chosen generator; the electronic control interface can then track the maximal productivity

by the coordinated results.

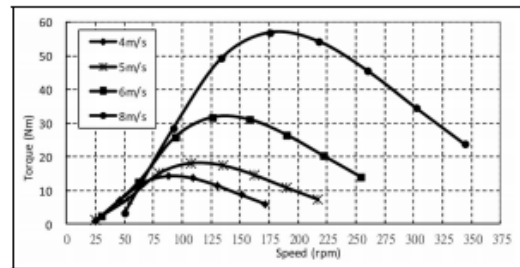


**Figure 6.** The  $T$  (torque)– $N$  (r/min) curves at different wind speeds.

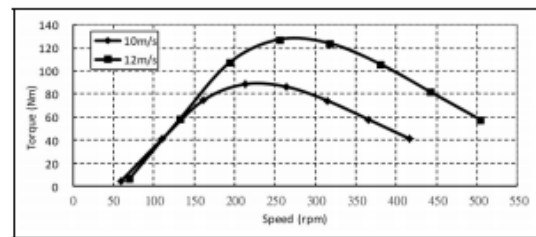


**Figure 7.** The  $T$  (torque)– $N$  (r/min) curves at different wind speeds.

The  $T$  (torque)– $N$  (r/min) bends of the turbine cutting edges, as per the CFD recreation, are plotted in Figures 6 and 7. It is likewise apparent from Figures 6 and 7 that when the inflow assault point surpasses the slow down edge, the edge torque will be lessened. The  $C_p$ –TSR bend is appeared in Figure 8. TSR is the proportion of the tip speed to the wind speed. Figure 8 demonstrates that when the TSR of the working point for this wind turbine is situated at 5–6.5, the cutting edges will work all the more effectively. For a wind turbine system, the torque

produced by the edges is utilized to conquer the torque of the generator.

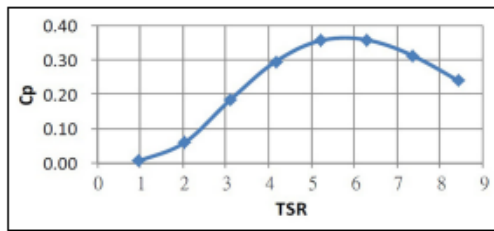


**Figure 8.** The  $C_p$ -TSR curve of the turbine blades.

Along these lines, the mechanical vitality can be exchanged to electronic vitality by the generator. In this manner, the information appeared in Figures 6 and 7 ought to be coordinated with those appeared in Figure 2. Figure 9 is gotten by consolidating Figures 6 and 2, and Figure 10 is gotten by consolidating Figures 7 and 2. From Figures 9 and 10, the working point (i.e. the coordinated point) at each wind speed can be resolved. At the ideal working point, both the efficiencies of turbine cutting edges and the generator ought to be kept high. The productivity of the turbine cutting edges differs with the dimensionless variable, as appeared in condition (2), TSR. As appeared in Figure 8, at the point when the TSR of the working point for this wind turbine is situated at 5–6.5, the cutting edges will turn out to be more proficient. In addition, it ought to be noticed that the working speed (r/min) can't be in the lofty incline locale of the chosen CV mode, as

appeared in Figure 3. In this steep slope area, the productivity of the generator will clearly be diminished. Along these lines, the criteria for the decision are working purposes of the TSR- $C_p$  bend as appeared in Figure 8, the productivity bends of the generator at each CV mode as appeared in Figure 3, the decided working speed (r/min), and the chose CV method of the generator. It is normal that the TSR esteem ascertained by in the high-effectiveness area of Figure 8 and not in the soak slant area of the chose CV mode in Figure 3.

***The situation when turbine sharp edges and generator are definitely not coordinated***

At the point when the two systems—sharp edge and generator—are unmatched, the generator will work at a similar CV mode for all wind speeds. For the situation where these two systems are not coordinated, a general CV mode ought to be chosen first. Here, the 280 V mode is picked in the unmatched case in light of the fact that the T-N bends of the turbine cutting edges at each wind speed can shape a crossing point with that of the 280 V mode, as appeared in Figure 11. At the crossing point, the torque required by the generator is equivalent to that created by the turbine sharp edges. Other CV modes

are not proposed in the unmatched case, aside from the 280 V modes.

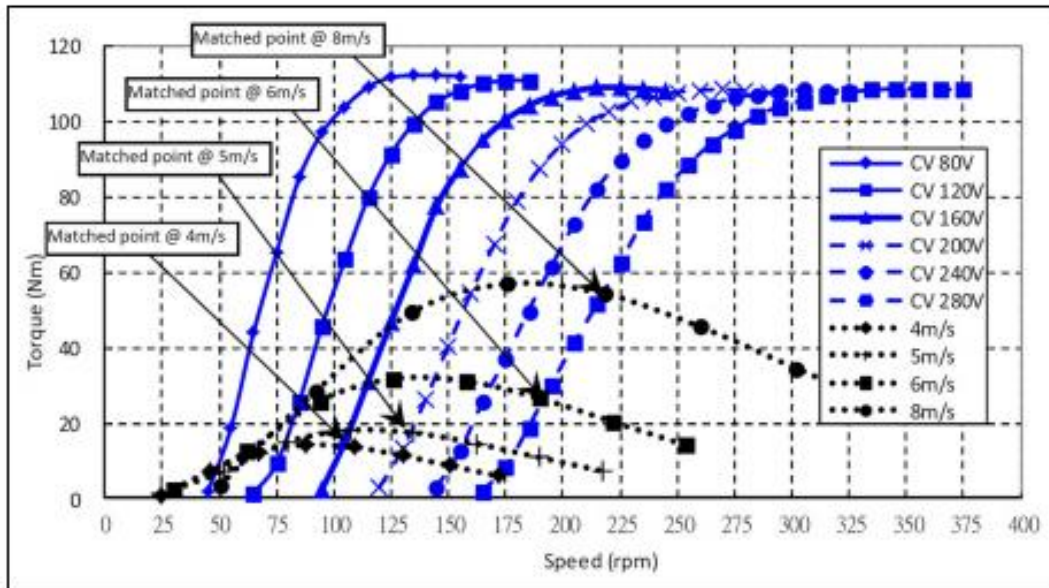


*Fig9 .he matching results of turbine blades and generator.*

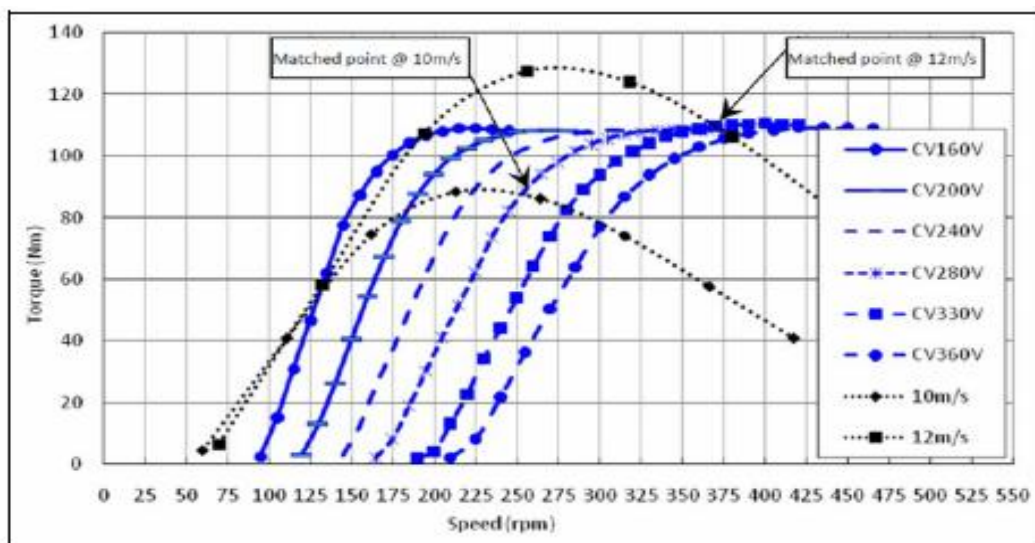


*Fig 10.matching results of turbine blades and generator*

In the event that the 200 V mode is chosen in the unmatched case, the turbine system will be overspeed at 10 m/s wind speed and some harm might be created on the grounds that the torque created by the

edges is much bigger than the generator requires (i.e. no crossing point is shaped at 12 m/s twist speed, as appeared in Figure 11).

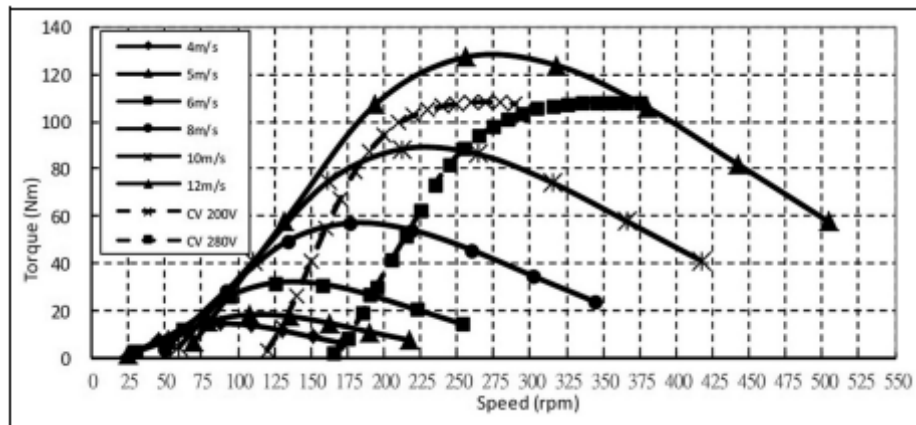


*Fig 11. The selection of the CV mode*

## CONCLUSION

The principle reason for this article was to build up a coordinating procedure for turbine cutting edges and generator to enhance the productivity of the wind turbine system. In view of the over, a few focuses can be finished up as takes after:

- 1) At various CV display, the T (torque)–N (r/min) bends of the generator are measured. The T (torque)–N (r/min) bends of turbine sharp edges are computed by CFD. Both the T (torque)–N (r/min) bends of the turbine sharp edges and the generator are plotted together to locate the ideal working focuses. The reason for picking the working focuses are the chosen CV method of the generator, the TSR–Cp bend of the turbine sharp edges, the productivity bends of the generator at each CV mode, and the decided working speed (r/min). It is

recommended that the decided cycles every moment be situated in the high efficiency area of the TSR–Cp bend of the turbine cutting edges, not in the precarious slant area of chosen CV mode.

- 2) By looking at the last yield force of the coordinated condition with that of the unmatched condition, it is realized that the last yield force of the coordinated condition at low wind speed, 4–5 m/s, will be expanded by 65%–44%, also, at high wind speed, 10–12 m/s, it will be expanded by 3%–5%.
- 3) The proposed strategy for accomplishing an ideal adjusts of turbine and generator is still in the formative stage. Overspeed security and commotion decrease amid the coordinating procedure are regions that warrant future exchange. The desire ought to be that the coordinated

pivoting speed is under control as the wind turbine encounters blasts and does not bring about unsuitable commotion.

The above concerns are proposed for future study to make this present procedure vigorous.

### Financing

The author(s) got no budgetary support for the exploration, initiation, as well as production of this article.

### REFERENCES

1. Glauert H. Plane propellers in streamlined hypothesis (ed WF Durand). New York: Dover, 1963.
2. Leishman JG. A semi-observational model for element slow down. *J Am Helicopter Soc* 1989; 34: 3–17.
3. Hirsch C. Numerical calculation of interior and outer streams. Chichester: Wiley, 1990.
4. Bardina JE, Huang PG and Coakley TJ. Turbulence demonstrating approval, testing, and improvement. NASA Specialized Memorandum No. 110446, 1997, [http://www.ewp.rpi.edu/hartford/;ferraj7/ET/Other/References/nasa\\_techmemo\\_110446.pdf](http://www.ewp.rpi.edu/hartford/;ferraj7/ET/Other/References/nasa_techmemo_110446.pdf)
5. Menter FR. Two-condition whirlpool consistency turbulence models for designing applications. *AIAA J* 1994; 32: 1598–1605.
6. Fingersh LJ, Simms D, Hand M, et al. Wind burrow testing of NREL's flimsy streamlined features analyze. In: 2001 ASME wind vitality symposium, Reno, NV, 11–14 January 2001, AIAA-2001-0035. Reston, VA: AIAA.
6. Hand MM, Simms DA, Fingersh LJ, et al. Insecure optimal design analyze stage VI: wind burrow test setups what's more, accessible information battles. NREL/TP-500- 29955, 2001. National Renewable Energy Laboratory, <http://www.nrel.gov/docs/fy02osti/29955.pdf>
7. Sørensen NN, Michelsen JA and Schreck S. Navierstokes forecasts of the NREL stage VI rotor in the NASA Ames 80ft 3 120 ft wind burrow. *Wind Energy* 2002; 5: 151–169.
8. Johansen J, Sørensen NN, Michelsen JA, et al. Withdrawn swirl reenactment of stream around the NREL stage VI rotor. *Wind Energy* 2002; 5: 185–197.
9. Modi A, Sezer-Uzol N, Long LN, et al. Versatile computational controlling for perception and control of expansive scale liquid progression reenactments. *J Aircraft* 2005; 42: 963–975.

10. Tongchitpakdee C, Benjanirat S and Sankar LN. Numerical reproduction of the optimal design of flat pivot twist turbines under yawed stream conditions. In: 43rd AIAA aviation sciences meeting and show, Reno, NV, 10–13 January 2005, AIAA 2005-773. Reston, VA: AIAA.
11. Sezer-Uzol N and Long LN. 3-D time-exact CFD reproductions of wind turbine rotor stream fields. AIAA Paper No. 2006-0394, 2006, <http://www.personal.psu.edu/lnl/papers/aiaawe2006-394.pdf>
12. Huang JC, Lin H, Hsieh TJ, et al. Parallel preconditioned WENO plot for three-dimensional stream recreation of NREL stage VI rotor. *Comput Fluids* 2011; 45: 276–282.
13. Van Dam C. Wind turbine streamlined features: reproduction approval. In: LANL 2011 wind designing workshop, Massachusetts, USA, 2–3 March 2011.
14. Li Y, Paik K-J, Xing T, et al. Dynamic overset CFD reenactments of wind turbine optimal design. *Restore Energ* 2012; 37: 285–298.
15. Villalpando F, Reggio M and Ilinca A. Numerical study of stream around frosted wind turbine airfoil. *EngApplComput Liquid Mech* 2012; 6: 39–45.
16. Sun H, Li J and Feng Z. Examinations on streamlined execution of turbine course at various stream conditions. *EngApplComput Fluid Mech* 2012; 6: 214–223.
17. Yelmule MM and EswaraRaoAnjuri VSJ. CFD expectations of NREL stage VI rotor tests in NASA/AMES wind burrow. *Int J Renew Energy Res* 2013; 3: 261–269.
18. Chamorro LP and Arndt RE. Non-uniform speed dispersion impact on as far as possible. *Wind Vitality* 2013; 16: 279–282.
19. Johnson B, Francis J, Howe J, et al. Computational actuator circle models for wind and tidal applications. *J Restore Energy* 2014; 2014: 172461 (10 pp.).
20. Kosasih B and Hudin HS. Impact of inflow turbulence force on the execution of uncovered and diffuseraugmented smaller scale wind turbine show. *Recharge Energ* 2016; 87: 154–167.
21. Yin XX, Lin YG, Li W, et al. Hydro-thick transmission based most extreme power extraction control for consistently variable speed twist turbine with improved effectiveness. *Reestablish Energ* 2016; 87: 646–655.
22. Tran TT and Kim DH. A CFD examine into the impact of flimsy

- streamlined obstruction on wind turbine surge movement. *Recharge Energ* 2016; 90: 204–228.
23. Koutroulis E and Kalaitzakis K. Plan of a most extreme control following system for wind-vitality change applications. *IEEE T Ind Electron* 2006; 53: 486–494.
24. Mirecki A, Roboam X and Richardiau F. Design unpredictability and vitality proficiency of little wind turbines. *IEEE T Ind Electron* 2007; 54: 660–670.
25. Odgaard PF, Larsen LFS, Wisniewski R, et al. On utilizing Pareto optimality to tune a straight model prescient controller for wind turbines. *Restore Energ* 2016; 87: 884–891